Marjorie A. Langell Publications   Published Research - Department of Chemistry

7-1-1999

Nickelocene adsorption on single-crystal surfaces

D. L. Pugmire
University of Nebraska-Lincoln, pugmire@ornl.gov

C. M. Woodbridge
University of Nebraska - Lincoln, cwoodbridge@ggc.edu

S. Root
University of Nebraska - Lincoln

Marjorie Langell
University of Nebraska - Lincoln, mlangell1@unl.edu

Nickelocene adsorption on single-crystal surfaces

D. L. Pugmire and C. M. Woodbridge
Departments of Chemistry and Center for Materials Research and Analysis, University of Nebraska-Lincoln, Lincoln, Nebraska 68588-0304

S. Root
Departments of Physics and Center for Materials Research and Analysis, University of Nebraska-Lincoln, Lincoln, Nebraska 68588-0304

M. A. Langell[a)]
Department of Chemistry and Center for Materials Research and Analysis, University of Nebraska-Lincoln, Lincoln, Nebraska 68588-0304

Nickelocene adsorption onto Ag(100), Ni(100), and NiO(100)/Ni(100) surfaces was studied with x-ray photoelectron spectroscopy and high-resolution electron energy loss spectroscopy at 135 K for monolayer and multilayer coverages of $NiCp_2$. On the relatively inert Ag(100) surface, nickelocene physisorbs molecularly, with its molecular axis perpendicular to the surface plane. Exposure to the reactive Ni(100) surface results in the decomposition of nickelocene into acetylene and acetylene-like fragments and, when this surface is warmed to 273 K, carbide contamination is observed. There is evidence for double-bond carbon on nickelocene-exposed NiO(100), and vinyl and propenyl fragments are the most likely decomposition products on this surface. At very large exposures, adsorbed nickelocene is molecularly condensed and, therefore, produces similar thin films on all three surfaces. © *1999 American Vacuum Society.* [S0734-2101(99)20904-9]

I. INTRODUCTION

The adsorption and subsequent decomposition of metallocenes at solid substrates are of interest to their proposed use as source molecules for the selective area deposition of metals.[1–12] Ferrocene, which is prototypical of the metallocenes, is generally very stable to thermal decomposition. Studies of ferrocene ($FeCp_2$; Cp=cyclopentadienyl) adsorbed onto several different substrates have been reported[1,3–8,12] and, for many of these, ferrocene is observed to adsorb molecularly but to undergo decomposition to lose cyclopentadiene under electron or photon irradiation at low temperatures. Warming the ferrocene-covered substrate to $\gtrsim 200$ K allows the material to desorb cleanly from areas that were not irradiated while depositing metal with features as small as 50 Å in the irradiated areas.[3]

Extension of this process to metallocenes containing more useful metals is desirable, but few studies have been reported for these materials to date. We present here adsorption studies of nickelocene ($NiCp_2$) on Ag(100), Ni(100), and NiO(100) surfaces, which span a range of reactivity in nickelocene decomposition. Nickelocene, with its 20 electron ligand valence shell, can be anticipated to be more reactive than the 18 electron ferrocene. The Ag(100) surface was chosen for investigation because it was expected to be relatively inert to metallocene decomposition. The quite reactive Ni(100) surface was studied as well. Finally, the NiO(100) surface with a reactivity anticipated to be intermediate between the other substrates was investigated. This last surface is also interesting because it is an insulating material, whereas the other surfaces are conductors.

II. EXPERIMENT

Ag(100) and Ni(100) single crystals were obtained from Goodfellow, oriented to within 0.5° of the (100) plane and polished to a mirror finish with 0.3 μm diamond paste. NiO(100) was grown as a thin film upon the Ni(100) substrate. Each metal substrate was mounted on a manipulator capable of resistive heating and liquid-nitrogen cooling, as described previously,[9] and the temperature of the sample was monitored with a type-K thermocouple (chromel-alumel). The manipulator was then placed into ultrahigh vacuum (UHV) in a stainless-steel bell jar equipped with Auger electron (AES) and x-ray photoelectron (XPS) spectroscopies, low-energy electron diffraction (LEED), and high-resolution electron energy loss spectroscopy (HREELS). While Auger spectroscopy could be used to monitor the clean substrates, exposure of nickelocene-covered surfaces to the AES primary electron beam resulted in electron-induced decomposition. Therefore, information on surface coverage was restricted to that obtained with XPS techniques. No x-ray or electron-induced decomposition of the metallocene was obvious during acquisition of XPS or HREELS data.

The Ag(100) sample was cleaned by repeated cycles of sputtering with Ar^+ (0.5 keV and 25 mA) at 623 K for 15 min followed by annealing under UHV at 673 K for 20 min until no impurities could be detected by AES. The Ni(100) sample was cleaned by repeated cycles of sputtering with Ar^+ (0.5 keV and 25 mA) at room temperature for 15 min, annealing under oxygen (1×10^{-7} Torr) for 15 min at 623 K and UHV annealing at 873 K for 5 min, similar to a previously reported cleaning procedure for Ni(100).[13] The latter cleaning procedure was also used to prepare the surface for the growth of the NiO(100) thin film. The clean Ni(100)

surface was then exposed to 600 L (5×10^{-7} Torr, 20 min) of O_2 and the substrate flashed to 573 K to convert the metastable NiO(111) to a NiO(100) film.[13] This dosing/heating procedure was repeated two more times to maximize the order and thickness of the film.

The clean surfaces were dosed by the admission of nickelocene vapor into the chamber through a standard leak valve equipped with a needle doser that concentrated the vapor in the vicinity of the sample crystals. During crystal exposure to $NiCp_2$ and the subsequent adsorbate analysis, crystal temperatures were maintained at 135 K unless otherwise noted. Exposures are reported in Langmuirs (L) and details of the doser time to langmuir calibration procedure can be found in Ref. 9.

XPS was performed with Mg $K\alpha$ radiation (1253.6 eV) and a Physical Electronics model 15-255 G double-pass cylindrical mirror analyzer operating in the constant pass energy, pulse-count mode. A pass energy of 50 eV was used during data collection. The binding energies were calibrated by reference to substrate transitions: 367.9 eV for Ag $3d_{5/2}$, 852.3 for Ni $2p_{3/2}$, and 529.4 eV for O $1s$ in NiO.

The high-resolution electron energy loss spectra were obtained using a LK-2000 spectrometer, a double-pass 127° sector electrostatic analyzer with variable detection angle capabilities. The primary electron beam was incident to the surfaces at 60° relative to the surface normal with a beam energy of 3.77 eV and a current of approximately 70 pA. The typical full width at half maximum (FWHM) for the spectra obtained ranged from 4 to 8 meV. A crystal bias of -1.7 eV was used in obtaining data on Ni(100) and NiO(100) substrates to ensure an adequate signal-to-noise ratio. No crystal bias was needed for Ag(100) measurements and the sample was simply grounded to the UHV chamber which served as common ground in the HREELS studies.

III. RESULTS AND DISCUSSION

A. Ag(100)

The vibrational spectrum of nickelocene adsorbed onto the Ag(100) substrate is shown in Fig. 1. Figure 1(b) contains the on and off specular HREELS data for high nickelocene exposures of 1500 L. The loss energies and assignments for all systems exhibiting molecular adsorption are listed in Table I. The spectrum is similar to infrared (IR) and Raman data previously reported for molecular nickelocene.[14] Thus as expected, at high exposures adsorbed nickelocene is a multilayered film of condensed material with surface properties exhibited by bulk $NiCp_2$. XPS measurements yield binding energies of 284.6 eV for the C $1s$ transition and 854.6 eV for the Ni $2p_{3/2}$ transition, in good agreement with literature values for molecular nickelocene.[15]

Figure 1(a) shows the on and off specular HREEL spectra for one monolayer of $NiCp_2$ interacting directly with the Ag(100) surface, produced by exposure to 11 L nickelocene at 135 K. The on specular spectrum shows modes at energies which are relatively unperturbed from vibrational modes observed for molecular $NiCp_2$ (Ref. 14) and for the multilayer
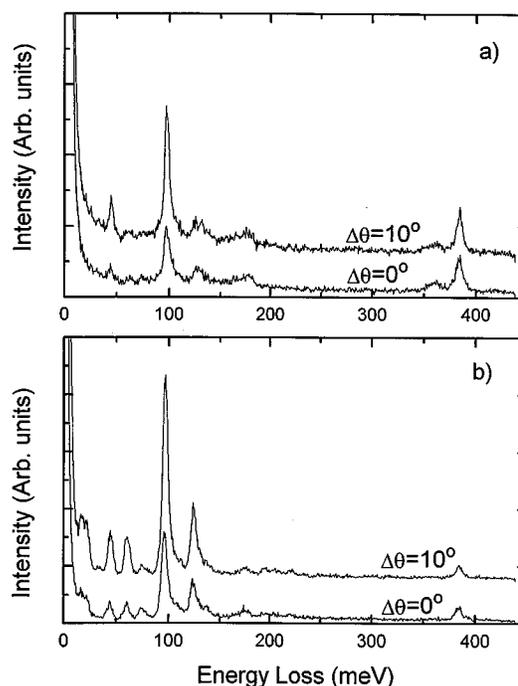

FIG. 1. Electron energy loss spectra of Ag(100) at 135 K exposed to (a) 11 L and (b) 1500 L of nickelocene. At high coverages the modes at 16.5 and 124.4 meV show an increase in relative intensity.

spectrum of Fig. 1(b). C $1s$ and Ni $2p_{3/2}$ XPS data, shown in Fig. 2, are found at 284.6 and 854.6 eV, respectively, and identical to binding energies obtained on the multilayer nickelocene condensate. The C $1s$/Ni $2p_{3/2}$ intensity ratio for the $NiCp_2$ monolayer is 0.35, which correlates with a 10/1 C/Ni atomic ratio when differences in the relative XPS cross sections are taken into account.[16] Upon warming the $NiCp_2$-covered Ag(100) substrate, the adsorbate desorbs cleanly to yield no carbon or nickel detectable by AES at 273 K. Thus, at the monolayer level, nickelocene is physisorbed on Ag(100) with no molecular decomposition evident.

Orientational information can be obtained on the molecular nickelocene by comparing on and off specular HREELS intensities. In the more stable staggered ring configuration, the nickelocene molecule belongs to the D_{5d} point group in which vibrational modes with A_{2u} or E_{1u} symmetries are expected to be dipole active. If the molecular axis of nickelocene is taken to be along the z direction, modes with E_{1u} symmetry will be polarized in the xy plane and A_{2u} modes will be polarized along the z axis. Depending on the orientation of the adsorbed molecules with respect to the surface, some or all of these potentially observable modes are also predicted to be dipole active by surface dipole selection rules, depending upon the orientation of the z axis with respect to the surface normal.

There are four characteristic modes which are particularly useful for the determination of the orientation of adsorbed nickelocene on the Ag(100) surface. The first of these modes is the ring-metal-ring bending mode with E_{1u} symmetry. The second is the asymmetric ring-metal-ring stretch, ν_{as}(RMR), with A_{2u} symmetry. The third is a mode in which C–H bend-

TABLE I. Energy losses and assignments for the molecular adsorption of nickelocene on various surfaces.

Molecular nickelocene	Ag(100)-monolayer meV (cm^{-1})	Ag(100)-multilayer meV (cm^{-1})	Ni(100)-multilayer meV (cm^{-1})	NiO(100)-multilayer meV (cm^{-1})
R–M–R bend	N.R.[a]	16.5(133)	N.R.	N.R.
R–M–R asymmetric stretch	45.1(364)	44.5(359)	45.7(369)	45.1(364)
Ring deformation[b]	61.0(492)	60.4(487)	60.4(487)	N.R.
Fuchs–Kliewer phonon				66.5(536)
C–H bend ($\perp$)	96.9(781)	97.0(782)	96.9(781)	96.3(777)
C–H bend ($\parallel$)	123.8(998)	124.4(1003)	125.0(1008)	125.0(1008)
Asymmetric C–C stretch	176.8(1426)	173.9(1403)	176.2(1421)	176.8(1426)
C–H stretch	386.7(3119), 360.3(2906)	384.3(3099)	385.3(3107)	384.7(3103)

[a]N.R. indicates modes that were not resolved.
[b]Tentative assignment.

ing occurs perpendicular to the plane of the rings with A_{2u} symmetry. The fourth is an additional C–H bending mode, with the motion in the plane of the rings in E_{1u} symmetry. Literature IR values for the energies of these modes are 15.5, 44.0, 95.9, and 124.0 meV (125, 355, 773, 1000 cm^{-1}), respectively.[14] At one monolayer coverage of NiCp$_2$ on Ag(100), all of these modes, except the ring-metal-ring bending mode, are observed.

Comparison of on and off specular data shows that the two modes with A_{2u} symmetry are dipole active by the dramatic loss of intensity at 10° off specular. The observed mode with E_{1u} symmetry is considerably less intense than the dipole modes on specular, and does not change significantly in intensity as the detection angle is moved off specular. The off specular behavior of this mode and the lack of

intensity of the two E_{1u} modes is evidence that vibrations with this symmetry must be oriented parallel to the surface plane. This indicates that nickelocene molecules on a Ag(100) surface at 135 K are adsorbed with the molecular axis perpendicular, or very nearly perpendicular, to the surface.

The intensities of all the modes observed at one monolayer increase as the exposure to nickelocene is increased. However, the two modes with E_{1u} symmetry show a more dramatic increase in intensity than the other modes observed in the HREEL spectrum. At high coverages, the ν_{as}(RMR) and the perpendicular C–H bending modes are observed as intense losses, as found for monolayer-covered Ag(100). Unlike the monolayer spectrum, the ring-metal-ring bending and in-plane C–H bending modes are also observed as intense losses at 16.5 (133) and 124.4 meV (1003 cm^{-1}), respectively. All four modes, with A_{2u} or E_{1u} symmetry, are dipole active in multilayer spectra, as seen when comparing the on specular data with that obtained off specular. Thus, at high coverages, the molecular axis of adsorbed nickelocene is neither strictly perpendicular to the surface, as it is for monolayer coverage, nor is it parallel to the surface but is at some intermediate angle.

B. Ni(100)

With long exposures of nickelocene to the Ni(100) substrate at 135 K, the HREEL spectrum [Fig. 3(b)] of the multilayer condensate resembles that of molecular nickelocene, as is found above for Ag(100). After exposure of the Ni(100) surface to 1200 L of nickelocene, the spectrum has many of the same features of Fig. 1(b), with the intense ν_{as}(RMR), perpendicular C–H bending, and parallel C–H bending modes observed at 45.7 (369), 96.9 (781), and 125.0 meV (1008 cm^{-1}), respectively. The photoelectron binding energies are similar to those seen in previous XPS data, with the C 1s transition at 284.5 eV. Photoemission from Ni 2p$_{3/2}$ core level of the nickelocene is not resolvable from the much stronger signal of the Ni(100) substrate.

A profound difference is seen, however, in the low coverage vibrational spectrum of nickelocene on Ni(100), which is evidently a more reactive substrate in metallocene decom-
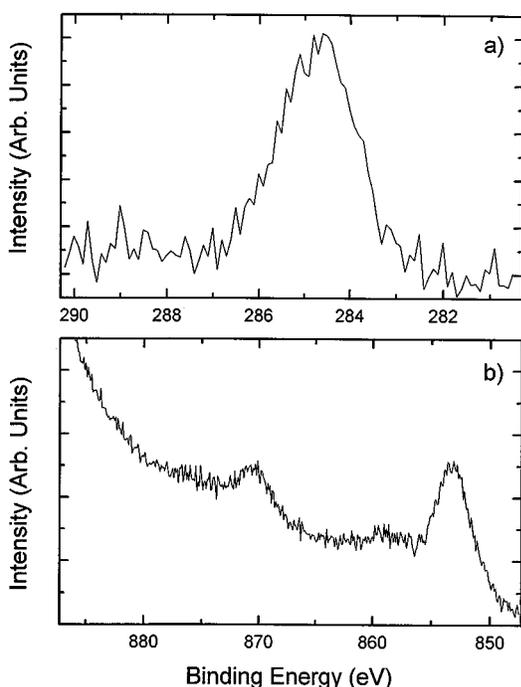

FIG. 2. XP spectra of one monolayer of nickelocene on Ag(100) at 135 K. (a) C 1s and (b) Ni 2p regions.
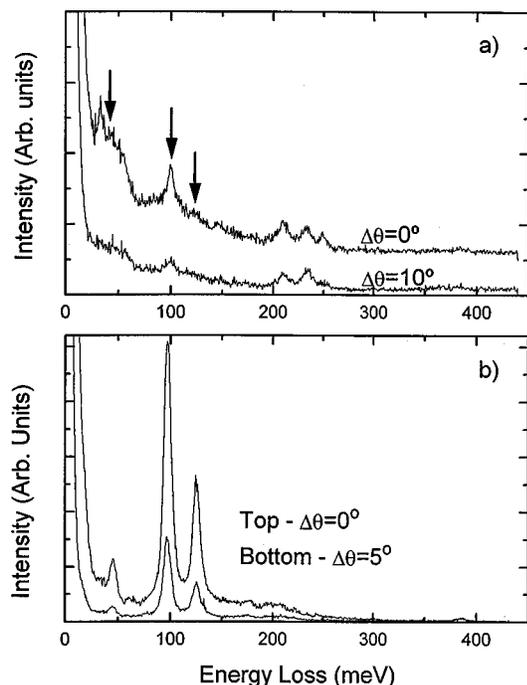
FIG. 3. Electron energy loss spectra of Ni(100) at 135 K exposed to (a) 8 L and (b) 1200 L of nickelocene. The low coverage spectra show considerable decomposition. The arrows indicate the losses due to nickelocene vibrational modes.

position than is the Ag(100) surface. Figure 3(a) shows the on and off specular HREEL spectra of the Ni(100) surface at 135 K exposed to 8 L of $NiCp_2$. Tentative spectral assignments for systems showing nickelocene decomposition are given in Table II. The three losses indicated with arrows in Fig. 3(a), occur at comparable energies to those observed for molecular nickelocene; thus there is some molecularly adsorbed $NiCp_2$ present on this surface. These modes are located at 43.3 (349), 100.0 (807), and 121.9 meV (983 cm^{-1}) and are due to the ν_{as}(RMR), C–H bend ($\perp$), and C–H bend ($\parallel$) vibrations of the nickelocene molecule. These modes are shifted slightly from multilayer nickelocene and from monolayer nickelocene on Ag(100), which may be an indication

that the adsorbate may be interacting more strongly on Ni(100). However, these modes belong to an adsorbate species that is still essentially molecular $NiCp_2$.

Three new losses appear in the monolayer spectrum and are observed in the 200–250 meV (1613–2016 cm^{-1}) range. This energy region is dominated by the stretching modes of CO, which may result from background contamination, and by species containing carbon–carbon triple bonds. No other possible adsorbate species that could potentially form from metallocene decomposition at 135 K is commonly encountered in this region. The mode observed at 249.4 meV (2011 cm^{-1}) is dipole active and is most likely due to CO. The ν_{CO} loss has previously been reported as 253.8 meV (2047 cm^{-1}) on Ni(100).[17]

The remaining two modes in this region, at 209.7 (1691) and 234.1 meV (1888 cm^{-1}), which are not dipole active, are due to ν_{CC} modes of acetylene or acetylene-like fragments that have strong C–C triple bond character. While exact identification of these species awaits more detailed HREELS and thermal desorption analysis, tentative assignments can be made by comparison of loss energies with those of IR spectra from organometallic compounds. In nickel coordination compounds, the stretching energies of carbon–carbon triple bond-containing ligands have been shown to fall in the 230–270 meV (1855–2178 cm^{-1}) region, with larger substituent groups having higher vibrational loss energies.[18] The lower of the two ν(C≡C) losses is assigned to acetylene. Several metal complexes with π-bonded acetylenic groups have been reported with the C–C stretching energy in the region of 200–220 meV (1613–1774 cm^{-1}).[19] The higher ν(C≡C) loss is assigned to propyne or a propyne-like fragment which contains a CH$_x$ substituent attached to one of the triple-bonded carbons. It, therefore, appears that on the Ni(100) surface the cyclopentadienyl ligand is decomposing into C$_2$H$_x$ and C$_3$H$_x$ acetylene-like fragments. The loss observed at 144.5 meV (1165 cm^{-1}) in Fig. 3(a) is due to a ν_{CC} mode of a carbon–carbon single bond,[20] and is assigned to the species giving rise to the higher energy ν(C≡C) found at 234.1 meV (1888 cm^{-1}). The losses at 34.1 (275) and 54.3 meV (438 cm^{-1}) are typical of metal–carbon stretches. The

TABLE II. Energy losses and assignments for decomposition fragments following the adsorption of nickelocene on Ni(100) and NiO(100) at 135 K.

Ni(100)-8 L	meV (cm^{-1})	NiO(100)-10 L	meV (cm^{-1})
M–C stretch	34.1(275)	M–C stretch	38.4(310)
R–M–R asymmetric stretch ($NiCp_2$)	43.3(349)	1st NiO phonon loss	67.1(541)
M–C stretch	54.3(438)	C–C stretch of propenyl	115.2(929)
C–H bend ($NiCp_2$)($\perp$)	100.0(807)	2nd NiO phonon loss	129.8(1047)
C–H bend ($NiCp_2$)($\parallel$)	121.9(983)	C=C stretch (vinyl and propenyl)[a]	193.5(1561)
C–C stretch (propyne)	144.5(1165)	C–H stretch	383.5(3093)
C≡C stretch (acetylene)	209.7(1691)		
C≡C stretch (propyne)	234.1(1888)		
C≡O stretch	249.4(2011)		
C–H stretch	383.5(3093)		

[a]This loss occurs in the region of the 3rd NiO phonon loss, therefore it is difficult to accurately determine the energy.
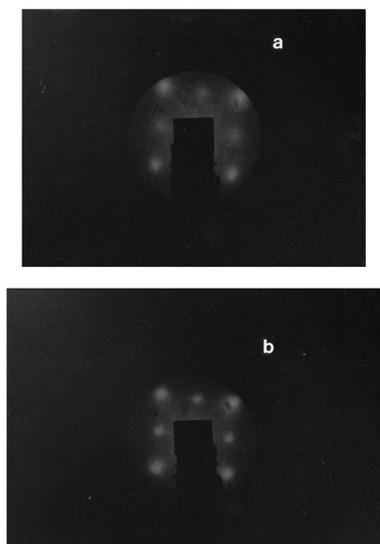
FIG. 4. LEED patterns of (a) the clean Ni(100) surface and (b) the NiO(100) thin film. Both pictures are taken with an incident energy of 69.8 eV.
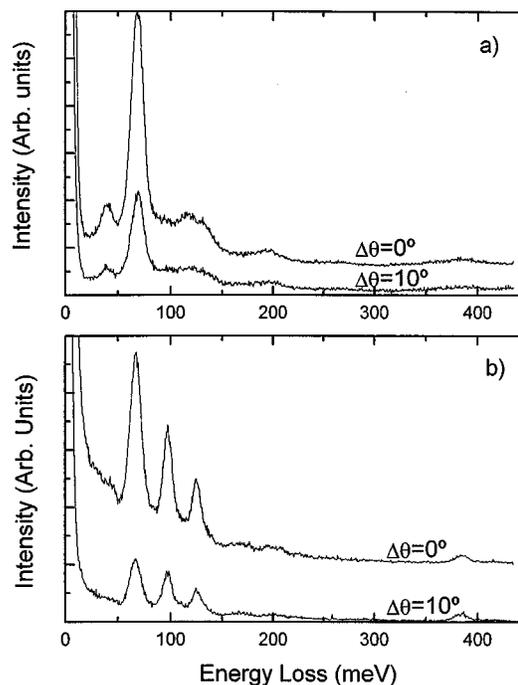

FIG. 5. Electron energy loss spectra of Ni(100)/NiO(100) at 135 K exposed to (a) 10 L and (b) 600 L of nickelocene. The intense loss at 67.1 meV is due to the Fuchs–Kliewer phonon of the metal oxide thin film.

ν_{MC} is reported at 28.5 (230) and 53.3 meV (430 cm^{-1}) for acetylene adsorbed on Ni(100).[21]

Despite the differences in the vibrational spectra upon moving to a more reactive surface, the binding energies seen with XPS are indistinguishable from those of molecular nickelocene. The carbon 1s transition is located at 284.3 eV and the energy of the nickel 2$p_{3/2}$ transition cannot be determined because of the large intensity of this transition in the substrate. The similarity of the XP spectra of the molecularly adsorbed nickelocene on Ag(100) and the decomposition products of nickelocene on Ni(100) is expected because of the difficulty in differentiating aromatic from aliphatic carbon with XPS.

AES data of the surface after it was heated to 273 K indicated the presence of carbon. The carbon line shape in the differentiated spectrum was characteristic of a carbide.[22] A small peak occurring at 283.7 eV was observed in the XPS data of the heated surface. The lower than typical binding energy of this carbon 1s XPS data also indicates the presence of a carbide.[16]

C. NiO(100)

NiO(100) was formed as a thin, crystalline film on the Ni(100) substrate. The growth and surface characteristics of Ni(100)/NiO(100) thin film substrates have previously been well studied.[13,23–27] The growth of the ordered thin film of NiO(100) on the Ni(100) substrate was monitored with several techniques. HREELS was used to detect the characteristic Fuchs–Kliewer phonon at 69.6 meV (561 cm^{-1})[13] described more fully below. Upon growth of the NiO thin film, XPS showed the characteristic shift of the Ni 2$p_{3/2}$ peak to 853.3 eV, an increase in the Ni 2$p_{3/2}$ satellite peak intensity, and the appearance of an O 1s photoelectron peak set to 529.4 eV by the calibration procedure. Figure 4 shows LEED patterns obtained of (a) the Ni(100) substrate and (b) the

NiO(100) thin film grown on the substrate. The reciprocal lattice spacing decreases for the oxide film, as expected, and the oxide film is thick enough to attenuate detection of the Ni(100) substrate in both XPS and LEED.

As found for multilayer nickelocene above, the vibrational spectrum taken after a high exposure of NiCp$_2$ resembles the condensed-film, molecular spectra. The HREEL spectrum of the NiO(100) thin film at 135 K exposed to 600 L of nickelocene is shown in Fig. 5(b). The ν_{as}(RMR) mode at 45.1 meV (364 cm^{-1}) appears as a small shoulder to the elastic peak. The intense mode at 66.5 meV (536 cm^{-1}) is due to NiO phonon loss and those at 96.3 (777 cm^{-1}) and 125.0 meV (1008 cm^{-1}) are due to the perpendicular and parallel C–H bending modes, respectively. XPS gives a carbon 1s binding energy of 284.5 eV, similar to data from high exposures to the other surfaces and to molecular nickelocene values.[15]

Adsorption of NiCp$_2$ on the NiO(100) thin film yields different results than found for either Ag(100) or Ni(100) substrates. The HREEL spectra obtained from the NiO(100)/Ni(100) substrate exposed to 10 L of nickelocene are shown in Fig. 5(a). The peaks occurring at 67.1 (541) and 129.8 meV (1047 cm^{-1}) are due to single and double energy Fuchs–Kliewer phonon losses of the nickel oxide substrate. The possibility of triple phonon loss, anticipated at approximately 200 meV (1613 cm^{-1}) but with considerably less intensity than the second phonon loss, unfortunately complicates the assignment of cyclopentadienyl surface fragments in this region. Despite these limitations, decomposition is clearly evident in the HREEL spectrum by the lack of the characteristic energy losses of molecular nickelocene. How-

ever, C–C triple bond loss modes are not evident in the spectrum, as is found for nickelocene decomposition on the Ni(100) substrate. The mode observed at 193.5 meV (1561 cm^{-1}) is most likely due to the C–C stretch of a carbon–carbon double bond only weakly interacting with the surface and thus still containing significant sp^2 character. Metal-vinyl compounds, in which the ligand is σ-bonded to the metal, are observed near 200 meV (1613 cm^{-1})[19] and the 193.5 meV (1516 cm^{-1}) loss is in agreement with the formation of σ-bonded vinyl and propenyl adsorbate species. The 115.2 meV (929 cm^{-1}) loss is tentatively assigned to the ν_{CC} of a single bond from the propenyl species, loss energies from which typically occur in the range of 115–120 meV (927–968 cm^{-1}).[20] The low energy loss at 38.4 meV (310 cm^{-1}) would then result from the carbon–metal stretch mode.

XPS C $1s$ data for this system are similar to that for aliphatic carbon, with the binding energy found at 284.5 eV. Upon warming to 273 K, all carbon-containing adsorbate species desorb and no carbon can be detected upon this system by AES/XPS techniques. Since ethylene does not adsorb on NiO(100) unless a significant number of defects are introduced into the system,[28] these results are consistent with the decomposition of nickelocene into vinylic and propenylic fragments observed in the HREEL spectrum and with their clean desorption as the system is warmed to room temperature.

IV. CONCLUSIONS

Adsorption of nickelocene on three surfaces with varying reactivity has been studied at 135 K. Nickelocene is molecularly physisorbed on the relatively inert Ag(100) substrate. The Ag(100) surface also allows for clean desorption upon heating to 273 K. In contrast, the reactive Ni(100) surface shows decomposition of adsorbed NiCp$_2$ into acetylene and acetylene-like fragments. Heating of the decomposition products on the surface results in some residual carbidic carbon. Double-bonded carbon containing species such as vinylic and propenylic fragments are observed when nickelocene is exposed to a NiO(100) surface, and upon heating to 273 K, these species desorb from the substrate. When exposed to large amounts of nickelocene, all three systems formed multilayers of condensed, molecular nickelocene.

[1]D. Welipitiya, A. Green, J. P. Woods, P. A. Dowben, B. W. Robertson, D. Byun, and J. Zhang, J. Appl. Phys. **79**, 8730 (1996).
[2]D. Welipitya, C. Wadfried, P. A. Dowben, I. Goblukoglu, and B. Robertson (unpublished).
[3]W. W. Pai, J. Zhang, J. F. Wendelken, and R. J. Warmack, J. Vac. Sci. Technol. B **15**, 785 (1997).
[4]R. Zanoni, M. N. Piancastelli, M. Marsi, and G. Margaritondo, J. Electron Spectrosc. Relat. Phenom. **57**, 199 (1991).
[5]F. Thibaudau, J. R. Roche, and F. Salvan, Appl. Phys. Lett. **64**, 523 (1994).
[6]L. M. Dyagileva, Russ J. Phys. Chem. **67**, 1071 (1993).
[7]H. D. Kaesz, R. S. Williams, R. F. Hicks, J. I. Zink, Y.-J. Chen, H.-J. Müller, Z. Xue, D. Xu, D. K. Shuh, and Y. K. Kim, New J. Chem. **14**, 527 (1990).
[8]J. T. Spencer, Prog. Inorg. Chem. **41**, 145 (1994).
[9]D. L. Pugmire, C. M. Woodbridge, and M. A. Langell, Surf. Sci. **411**, L844 (1998).
[10]D. Welipitiya, C. N. Borca, C. Waldfried, C. Hutchings, L. Sage, C. M. Woodbridge, and P. A. Dowben, Surf. Sci. **393**, 34 (1997).
[11]O. Henrion and W. Jaegermann, Surf. Sci. **387**, L1073 (1997).
[12]F. Thibaudau, L. Masson, A. Chemam, J. R. Roche, and F. Salvan, J. Vac. Sci. Technol. A **16**, 2967 (1998).
[13]M. A. Langell, C. L. Berrie, M. H. Nassir, and K. W. Wulser, Surf. Sci. **320**, 25 (1994).
[14]E. R. Lippincott and R. D. Nelson, Spectrochim. Acta **10**, 307 (1958).
[15]M. Barber, J. A. Connor, L. M. R. Derrick, M. B. Hall, and I. H. Hillier, J. Chem. Soc., Faraday Trans. 2 **69**, 559 (1973).
[16]*Handbook of X-Ray Photoelectron Spectroscopy*, edited by G. E. Muilenberg (Perkin–Elmer Corporation, Eden Prairie, MN, 1979).
[17]J. Lauterbach, M. Wittmann, and J. Küppers, Surf. Sci. **279**, 287 (1992).
[18]D. M. Adams, *Metal-Ligand and Related Vibrations* (St. Martin's Press, New York, 1968), p. 212.
[19]K. Nakamoto, *Infrared and Raman Spectra of Inorganic and Coordination Compounds*, 5th ed. (Wiley, New York, 1997), pp. 263, 282.
[20]T. Shimanouchi, *Tables of Vibrational Frequencies*, Consolidated Vol. I, NSRDS-NBS 39; Vol. II, J. Phys. Chem. Ref. Data **6**, 993 (1977).
[21]F. Zaera and R. B. Hall, J. Phys. Chem. **91**, 4318 (1987).
[22]M. A. Smith, S. Sinharoy, and L. L. Levenson, J. Vac. Sci. Technol. A **16**, 462 (1979).
[23]M. Bäumer, D. Cappus, H. Kuhlenbeck, H.-J. Freund, G. Wilhelmi, A. Brodde, and H. Neddermeyer, Surf. Sci. **253**, 116 (1991).
[24]C. Xu, D. W. Goodman, J. Chem. Soc., Faraday Trans. **91**, 3709 (1995).
[25]R. S. Saiki, A. P. Kaduwela, J. Osterwalder, C. S. Fadley, and C. R. Brundle, Phys. Rev. B **40**, 1586 (1989).
[26]R. B. Hall, C. A. Mims, J. H. Hardenbergh, and J. G. Chen, ACS Symp. Ser. **482**, 85 (1992).
[27]W.-D. Wang, N. J. Wu, and P. A. Thiel, J. Chem. Phys. **92**, 2025 (1990).
[28]R. P. Furstenau and M. A. Langell, Surf. Sci. **159**, 108 (1985).